

First-principles studies of Mn-doped LiCoPO₄*

Lin Zhi-Ping(林志萍)^{a)b)}, Zhao Yan-Ming(赵彦明)^{a)†}, and Zhao Yu-Jun(赵宇军)^{a)}

^{a)}Department of Physics, South China University of Technology, Guangzhou 510640, China

^{b)}School of Physics, Guangdong University of Technology, Guangzhou 510090, China

(Received 20 November 2009; revised manuscript received 7 June 2010)

This paper investigates Mn-doped LiCoPO₄ material using first-principles calculations. Results indicate that the volume change of LiMn_xCo_{1-x}PO₄ to Mn_xCo_{1-x}PO₄ is smaller than that of undoped LiCoPO₄, which is responsible for the excellent tolerance of repeated cycling in lithium ion batteries. Combining first-principles calculations with basic thermodynamics, we calculate the average intercalation voltage of Mn-doped LiCoPO₄. It is shown that the redox couple Mn³⁺/Mn²⁺ can be observed with increasing Mn content. Therefore, the Mn ion displays some electrochemical activity during discharge/charge of LiMn_xCo_{1-x}PO₄ due to the coexistence of Co and Mn.

Keywords: first-principles calculation, electrochemical activity doping

PACS: 82.47.Aa, 71.15.Nc, 71.15.Mb, 71.20.Be

DOI: 10.1088/1674-1056/20/1/018201

1. Introduction

In recent years there has been interest in the use of lithium transition metal phosphates with olivine structure LiMPO₄ ($M=Fe, Mn$ and Co) as potential cathode materials for Li-ion batteries.^[1-4] This crystalline structure has an orthorhombic unit cell with space group $Pmnb$, which accommodates four units of LiMPO₄. The distorted MO₆ octahedrons are corner shared and cross linked by the PO₄ tetrahedron and thus form a three-dimensional network. Their theoretical capacity of 170 mAh/g⁻¹ provides higher energy density than that of LiCoO₂.^[4] For LiFePO₄, it has been proved by molecular dynamics simulations that the diffusion channel of the Li ion is one-dimensional and the metal doped on Li-site will block the one-dimensional diffusion pathway.^[5-7] In addition, by doping with transition metal ions, the properties of these compounds can be improved.^[8-10] For example, Ni, Co, Mg, Rh doping in the Fe-site of LiFePO₄ can improve the capacity and the electronic conductivity of the material.^[10,11] The olivine type LiMPO₄ compounds and their solid solution system operate at 3.1–4.8 V versus Li/Li⁺. Padhi *et al.*^[1] reported that for the Li(Mn_yFe_{1-y})PO₄ solid solution system the width of the 4.1 V plateau (Mn³⁺/Mn²⁺) relative to that of the 3.4 V plateau (Fe³⁺/Fe²⁺) increases with increasing Mn content y . In other words, the charge and discharge potential of LiFePO₄ improves to 4.1 V by Mn doping due to the coexistence of Fe with Mn at the

octahedral 4c site in Li(Mn_yFe_{1-y})PO₄. The adoption of LiMnPO₄ takes account of the compatibility of its 4.1 V redox coupling of Mn³⁺/Mn²⁺ and its high energy density with present lithium-ion batteries. Satya Kishore and Varadaraju^[12] have studied Mn²⁺-doped LiCoPO₄ but the reductive peak at ~4.1 V from studying cyclic voltammograms (CV) was not obtained, which suggests that Mn²⁺ is not oxidised during de-intercalation of lithium from LiCo_{1-x}Mn_xPO₄. Therefore, the difference in the electrochemical properties of Mn in Mn-doped LiFePO₄ and Mn-doped LiCoPO₄ becomes apparent.

In this work, we perform first-principles calculations for the LiMn_xCo_{1-x}PO₄ system and investigate its crystal structure, electron structure, and average intercalation voltage in order to illuminate the electrochemical properties of Mn in Mn-doped LiCoPO₄.

2. Computational details

The calculations are based on density functional theory with the general gradient approximation (GGA) using the Perdew–Wang form for the exchange correlation energy^[13] as implemented in the Vienna *ab initio* Simulation Package (VASP).^[13-18] Doped systems are simulated by Mn atoms replacing Co atoms in an 84-atom super-cell. The interactions between valence electrons and ions are represented with the projector augmented wave (PAW) pseudo-potentials.

*Project supported by the National Natural Science Foundation of China (Grant No. 50772039) and the Science and Technology Bureau of Guangdong Province, China (Grant No. 07118058).

†Corresponding author. E-mail: zhaoym@scut.edu.cn or zhipinglphy@gdut.edu.cn

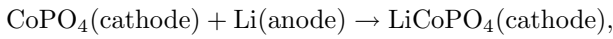
© 2011 Chinese Physical Society and IOP Publishing Ltd

<http://www.iop.org/journals/cpb> <http://cpb.iphy.ac.cn>

The wave functions are expanded in plane waves with an energy cutoff of 450 eV. Brillouin zone integration of the band structure is performed with a $2 \times 1 \times 4$ Monkhorst–Pack mesh. The formation energies are well converged to within 10^{-3} eV with respect to k -point integration. The Fermi level is smeared by the Gaussian method with a width of 0.2 eV. In order to obtain the orbital-projected electronic structure information, the Wigner–Seitz radii of 0.80, 1.40, 1.40, 1.20 and 1.20 Å (1 Å=0.1 nm) for Li, Mn, Co, P and O ion are adopted.

When more than one Co atom is replaced by Mn, 12 cobalt lattice sites result in multiple nonequivalent metal-doped configurations. To avoid computational complexity in the calculation of ΔE due to enormous doped configurations, we adopt a reasonable doping model to calculate the total energy and estimate the average intercalation voltage, which is described by Shi *et al.*^[19] This model suggests that two doped atoms are located as far as possible away from each other and the sum of the distance over all doped atoms should be maximised.

The average Li insertion potential could be obtained through total energy calculations.^[20,21] If ΔG_r is the Gibbs free energy for the reaction:



then the average insertion voltage is given by

$$\bar{V} = -\frac{\Delta G_r}{F}, \quad (1)$$

where F is the Faraday constant. Since the effects due to changes in volume and entropy are small, the Gibbs energy difference is approximated by the internal energy difference at 0 K, supplied by our first-principles total-energy calculations through

$$\Delta E_r = E_{\text{LiCoPO}_4} - E_{\text{Li}} - E_{\text{CoPO}_4}. \quad (2)$$

Here the cohesive energy of Li is calculated from its bcc structure, which corresponds to the structural phase of the Li anode.

3. Results and discussion

We perform the optimisation of spin structure and calculate the total energy for the ferromagnetic (FM), antiferromagnetic (AFM), as well as the nonmagnetic (NM) configurations, which are listed in Table 1 together with the relaxed lattice parameters. The result indicates that the AFM configuration shown in

Fig. 1 has the lowest total energy, which is lower than that of the NM and FM configurations by 0.64 eV and 0.47 eV, respectively. Therefore, the Co ions are AFM coupled in the ground state of the LiCoPO₄ system. This is in agreement with the ground state of LiFePO₄.^[22] In addition, it is noted that optimised lattice parameters for the calculated AFM configuration are in good agreement with the experimental values to within 1% error. Therefore, the stable AFM configuration is adopted in our following calculation of compounds with different Mn doping. For the Mn-doped LiFePO₄ system, Yamada *et al.*^[23] have confirmed that its AFM phase is not changed due to Mn doping.

Table 1. Relaxed lattice parameters of LiCoPO₄ and its total energy with different magnetic configurations.

	$a/\text{Å}$	$b/\text{Å}$	$c/\text{Å}$	$E/(\text{eV/f.u.})$
Expt.	10.202	5.922	4.699	
NM	9.816	5.869	4.691	-46.902
FM	10.126	5.918	4.719	-47.068
AFM	10.110	5.923	4.717	-47.542

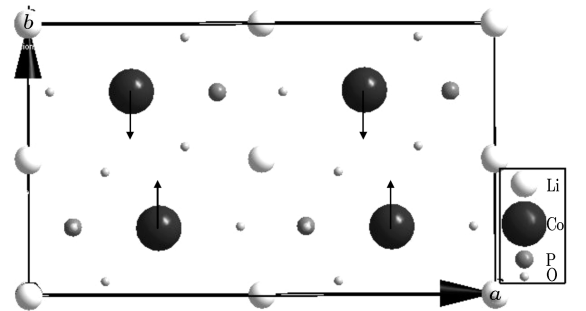


Fig. 1. The stable AFM spin configuration of LiCoPO₄.

The optimised lattice parameters and volume for the pure and Mn-doped LiCoPO₄ are shown in Figs. 2 and 3, together with the experimental values. The calculated volume of the unit cell is 0.68% smaller than the experimental value for LiCoPO₄, and is basically in agreement with the calculated result of Deniard *et al.*^[24] It is interesting to note that the lattice parameters a , b and c increase with increasing Mn concentration, which is in good agreement with the experimental investigation by Satya Kishore and Varadaraju.^[12] The increase in lattice parameters may enlarge the move channel of lithium ions and thus improve the ionic conductivity. It is also found that the crystalline structure is obviously distorted with increasing Mn content. This distortion was also found in Li(Mn _{y} Fe _{$1-y$})PO₄ compounds by Padhi *et al.*,^[1] and Deniard *et al.*,^[24] which is harmful

to the intercalation and deintercalation performance of the cathode material^[24] and assists the electronic conductive performance.^[25] The Mn doping affects not only the structure of lithiated compounds but also that of delithiated compounds. All the lattice parameters of delithiated compounds increase with increasing Mn content if we hypothesise that all lithium ions can be entirely extracted. The volume change for $\text{Mn}_x\text{Co}_{1-x}\text{PO}_4/\text{LiMn}_x\text{Co}_{1-x}\text{PO}_4$ with different x content is shown in Fig. 3.

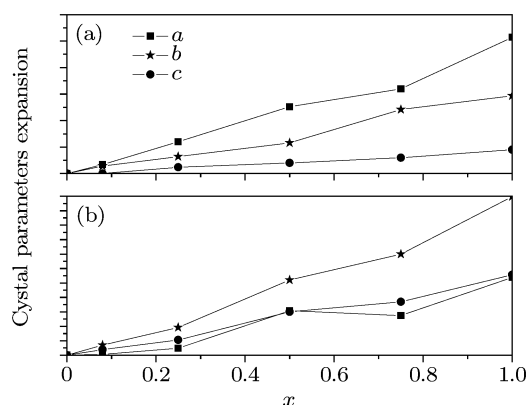


Fig. 2. Crystal parameter expansion of Mn doped structure with different x for (a) $\text{LiCo}_{1-x}\text{Mn}_x\text{PO}_4$ and (b) $\text{Co}_{1-x}\text{Mn}_x\text{PO}_4$.

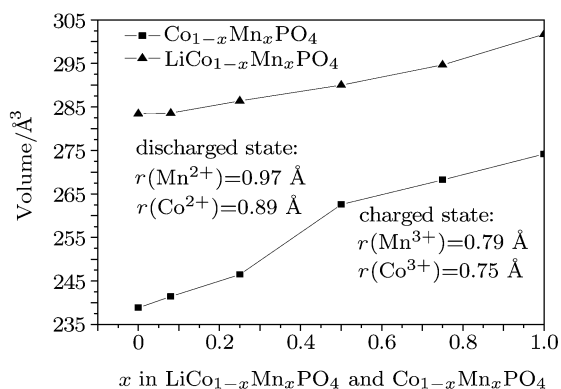


Fig. 3. Volume change of $\text{LiCo}_{1-x}\text{Mn}_x\text{PO}_4$ and $\text{Co}_{1-x}\text{Mn}_x\text{PO}_4$ with different x values.

It can be seen that the volume increases with increasing Mn content. The main reason is that the radii of Mn^{2+} (0.97 Å) and Mn^{3+} (0.79 Å) ions are larger than those of Co^{2+} (0.89 Å) or Co^{3+} (0.75 Å) ions. The volume change rate for Mn-doped compounds is smaller than that of $\text{CoPO}_4/\text{LiCoPO}_4$ (15.44%) and decreases with increasing Mn content. In other words, Mn doped systems are more stable than pure LiCoPO_4 during the lithium extraction/reinsertion process. It has been suggested by Bramnik *et al.*^[26] and Wolfenshtine *et al.*^[27] that the change of structure is responsible

for the fade of capacity. It is clear that the stability of the structure should be beneficial in improving the retention rate of capacity. It has been reported that a small amount of metal ion doping may improve the capacity delivery and cycle performance of the lithium ion battery.^[12,28,29] Hence, the tolerance of Mn-doped LiCoPO_4 can be improved during repeated cycling of lithium ion batteries.

Analysis of the electronic structure may provide insight into the characteristic features of cathode materials. In Fig. 4, we show the total electronic density of states (TDOS) for $\text{LiMn}_x\text{Co}_{1-x}\text{PO}_4$ for $x = 0, 0.08, 0.25, 0.50$ and 0.75 . It is found that the Fermi level lies in a band which is formed by hybridisation of cobalt d-states, phosphorus p-states and oxygen p-states. Therefore, these compounds show a metallic character, which illustrates the good electronic conductivity of the compounds during discharge/charge. For lithiated phases $\text{LiMn}_x\text{Co}_{1-x}\text{PO}_4$, the calculated TDOS curves are very similar to each other for various Mn concentrations. With increasing Mn content the conduction bands are shifted to the right, while the valence bands are shifted to the left according to the Fermi level and widen the width of the band gap above the top of the valence band.

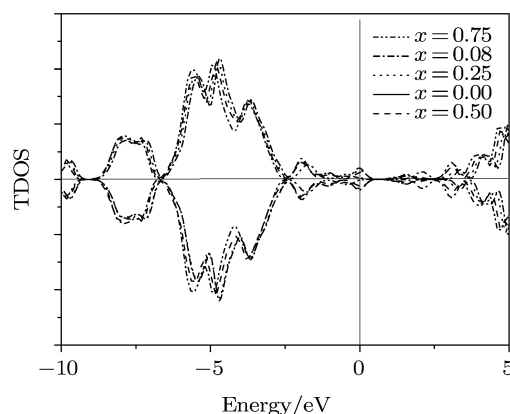


Fig. 4. Total density of states of $\text{LiCo}_{1-x}\text{Mn}_x\text{PO}_4$; the Fermi level is set as a reference.

In order to display the role of Co and doped Mn ions in compounds, Fig. 5 shows the partial density of states (PDOS) of Co and Mn ions for $\text{LiMn}_x\text{Co}_{1-x}\text{PO}_4$ for $x = 0.25, 0.50$ and 0.75 . It can be noted that the band near the Fermi level is dominated by $\text{Mn}_x\text{Co}_{1-x}$ d-states. By comparing the PDOS of Co and Mn ions with different Mn content, it can be found that the distribution of the Co and Mn d-states for $x = 0.5$ and 0.75 is similar and has a clear difference from that of Co and Mn d-states

for $x = 0.25$. For $x = 0.25$, electronic states near the Fermi level mainly come from the up-spin Mn d-states, but for $x = 0.5$ and 0.75 electronic states at the Fermi level come from mainly the up-spin Co d-states.

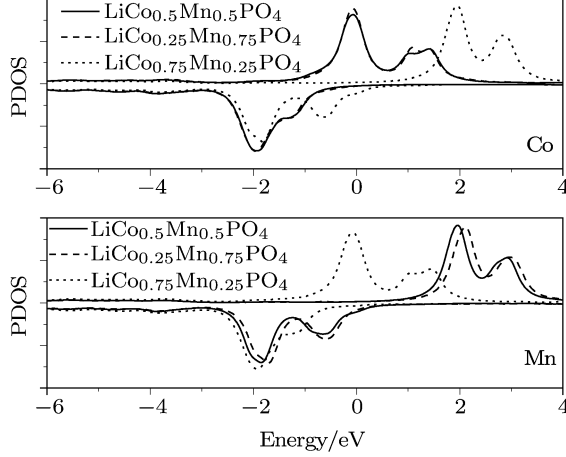


Fig. 5. The PDOS of Co and Mn atoms in $\text{LiCo}_{1-x}\text{Mn}_x\text{PO}_4/\text{Co}_{1-x}\text{Mn}_x\text{PO}_4$ for $x = 0.25, 0.5$ and 0.75 .

The Li insertion potential plays an important role in its application to the cathode material of rechargeable Li ion batteries. The calculated average intercalation voltages of the pure and Mn-doped LiCoPO_4 according to Eqs. (1) and (2) are listed in Table 2. They indicate that the GGA calculated result underestimates the average intercalation voltage by 1.3 eV with respect to experiment. But our result is basically in good agreement with the calculated result of Le Bacq and Pasturel^[30] using the GGA method. Therefore, the results calculated using the GGA method, which adopts a very approximate treatment of the electron correlation in transition metal orbitals, can reflect the voltage change

trend. From Table 2, it is found that the theoretical average intercalation voltage of the Mn-doped sample is about 3.48 eV when $x = 0, 0.08$ and 0.25 , which is in agreement with the redox couple $\text{Co}^{3+}/\text{Co}^{2+}$. In other words, Mn^{2+} is not oxidised during extraction of lithium from $\text{LiCo}_{1-x}\text{Mn}_x\text{PO}_4$ when $x \leq 0.25$, which is reflected by corresponding experimental results on $\text{LiMn}_x\text{Co}_{1-x}\text{PO}_4$.^[12] It was reported that the reduction potential $\text{Co}^{3+}/\text{Co}^{2+}$ peak in the CV profile of Mn-doped compounds is not changed and the reduction potential of $\text{Mn}^{3+}/\text{Mn}^{2+}$ in ~ 4.1 V is not observed in $\text{LiMn}_x\text{Co}_{1-x}\text{PO}_4$ when $x \leq 0.2$.^[12] When $x = 0.5$, the average intercalation voltage becomes 3.24 eV, which is lower than the redox couple $\text{Co}^{3+}/\text{Co}^{2+}$. By increasing Mn content to 0.75, the average voltage decreases 3.10 eV, which is in agreement with the redox couple $\text{Mn}^{3+}/\text{Mn}^{2+}$, and thus Mn^{2+} ions show electrochemical activity when $x = 0.75$. The average intercalation voltage 3.24 eV for $x = 0.5$ is the mixing of the redox couple $\text{Co}^{3+}/\text{Co}^{2+}$ and $\text{Mn}^{3+}/\text{Mn}^{2+}$, which shows that the Co and Mn ions display some electrochemical activity under $x = 0.5$. Therefore, the $\text{LiMn}_x\text{Co}_{1-x}\text{PO}_4$ solid solution structure satisfies a similar electrochemical charge and discharge characteristics to $\text{Li}_z\text{Fe}_{1-y}\text{Mn}_y\text{PO}_4$.^[31] The two-dimensional phase diagram of $\text{Li}_z\text{Fe}_{1-y}\text{Mn}_y\text{PO}_4$ shows the two-phase redox region with a potential of 4.1 V vs. Li/Li^+ when $x \geq 0.75$, and the redox region with a potential $\text{Co}^{3+}/\text{Co}^{2+}$ of 4.8 V vs. Li/Li^+ when $x \leq 0.25$ as well as the $\text{Mn}^{3+}/\text{Mn}^{2+}$ and $\text{Co}^{3+}/\text{Co}^{2+}$ redox co-existent region when $0.25 \leq x \leq 0.75$. Hence, the coexistence of Co and Mn can improve the electrochemical activity of Mn.

Table 2. Calculated lithium intercalation voltage for pure and Mn doped LiCoPO_4 . The experimental value for LiCoPO_4 is 4.8 eV (Ref. [2]).

x in $\text{LiCo}_{1-x}\text{Mn}_x\text{PO}_4$	0	0.08	0.25	0.50	0.75	1.00
Voltage/V	-3.48	-3.47	-3.49	-3.24	-3.10	-3.09

To examine the local charge transport with Mn doping, the calculated number of electrons of d-states around Co and Mn atoms are summarised in Table 3. It can be found that the number of electrons around Co and Mn atoms decreases with increasing Mn content. It illustrates that there is direct coupling between the 3d bands of Mn and Co. In the case of highest Mn doping, the number of electrons around the Mn and Co atoms changes by 0.031 e and 0.051 e, respectively. Based on the simple point-charge interaction approximation, the change of the intercalation voltage upon Mn doping can be estimated. The length of the Li-O bond is 2.11 Å (3.988 a.u.) and the distance between Li and metal is 3.03 Å (5.727 a.u.), 3.05 Å (5.765 a.u.) and 3.06 Å (5.783 a.u.) for $x = 0.25, 0.5, 0.75$, respectively. Therefore, according to the simple point-charge model (assuming Li ionicity of +1), the total energy difference ΔE between $\text{LiCo}_{1-x}\text{Mn}_x\text{PO}_4$ and LiCoPO_4 may be

written as follows:

$$\Delta E = 4 \times N \times \left[\frac{1}{3.988} - \frac{1}{\text{bondlength}_{\text{Li-Metal}}} \right] \text{hartree},$$

where N is the average transferred charge number of the metal atoms. The results are shown in Table 3. They show that the intercalation voltage of $\text{LiCo}_{1-x}\text{Mn}_x\text{PO}_4$ decreases by 0.018, 0.15 and 0.35 V, respectively. This is in agreement with 0.01, 0.24 and 0.38 V given by first-principles total-energy calculations. Hence, from the viewpoint of charge transport, the decrease of average intercalation voltage with increasing Mn content is due to the fact that there are some charges transferred between metal and oxygen, and the energy change is due mostly to the Coulombic interaction between ions.

Table 3. Number of electrons around Co and Mn ions as well as the total energy difference ΔE between $\text{LiCo}_{1-x}\text{Mn}_x\text{PO}_4$ and LiCoPO_4 .

x	0.00	0.08	0.25	0.50	0.75
Co	8.044 e	8.047 e	8.043 e	8.024 e	8.013 e
Mn		5.761 e	5.755 e	5.739 e	5.710 e
$\Delta E/\text{eV}$			0.018	0.17	0.35

4. Conclusion

In this paper, the electronic structure of Mn-doped LiCoPO_4 is investigated using first-principles calculations. The results display that the lattice parameters ' a ' and ' b ' increase with increasing Mn content and there is insignificant change in the ' c ' parameter; the change of lattice parameter is in good agreement with experimental investigation. It is found that the volume change of $\text{LiMn}_x\text{Co}_{1-x}\text{PO}_4$ to $\text{Mn}_x\text{Co}_{1-x}\text{PO}_4$ is smaller than that of pure LiCoPO_4 material, which is beneficial in improving the retention rate of capacity. Combining first-principle calculations

with basic thermodynamics, the average intercalation voltage of Mn-doped LiCoPO_4 is calculated. It can be seen that the redox couple $\text{Co}^{3+}/\text{Co}^{2+}$ is dominant when $x < 0.25$ and with increasing Mn content the redox couple $\text{Mn}^{3+}/\text{Mn}^{2+}$ is also found. Therefore, It illustrates that the discharge/charge properties in $\text{LiMn}_x\text{Co}_{1-x}\text{PO}_4$ and $\text{LiFe}_{1-y}\text{Mn}_y\text{PO}_4$ are similar: the manganese can display some electrochemical activity under the coexistence of Co and Mn. In addition, the change of intercalation voltage upon Mn doping is estimated by the simple point-charge model, which also gives the same varying trend.

References

- [1] Padhi A K, Nanjundaswamy K S and Goodenough J B 1997 *J. Electrochem. Soc.* **144** 1188
- [2] Amine K, Yasuda H and Yamachi M 2000 *Electrochem. Solid-State Lett.* **3** 178
- [3] Carrasco J, Lopez N and Illas F 2004 *Phys. Rev. Lett.* **93** 225502
- [4] Yamada A and Chung S C 2001 *J. Electrochem. Soc.* **148** A960
- [5] Ouyang C Y, Shi S Q, Wang Z X, Huang X J and Chen L Q 2004 *Phys. Rev. B* **69** 104303
- [6] Ouyang C Y, Shi S Q, Wang Z X, Li H, Huang X J and Chen L Q 2004 *J. Phys.: Condens. Matter* **16** 2265
- [7] Ouyang C Y, Shi S Q, Fang Q and Lei M S 2008 *J. Power Sources* **175** 891
- [8] Shi S Q, Ouyang C Y, Wang D S, Chen L Q and Huang X J 2003 *Solid State Communications* **126** 513
- [9] Shi S Q, Ouyang C Y, Lei M S and Tang W H 2007 *J. Power Sources* **171** 908
- [10] Wang D Y, Li H, Shi S Q, Huang X J and Chen L Q 2005 *Electrochimica Acta* **50** 2955
- [11] Ouyang X F, Shi S Q, Ouyang C Y, Jiang D Y, Liu D S, Ye Z Q and Lei M S 2007 *Chin. Phys.* **16** 3042
- [12] Satya Kishore M V V M and Varadaraju U V 2005 *Mater. Res. Bull.* **40** 1705
- [13] Kresse G and Joubert J 1999 *Phys. Rev. B* **59** 1758
- [14] Kresse G and Hafner J 1993 *Phys. Rev. B* **47** 558
- [15] Kresse G and Hafner J 1994 *Phys. Rev. B* **49** 14251
- [16] Kresse G and Hafner J 1994 *J. Phys.: Condens. Mater. Sci.* **6** 8245
- [17] Kresse G and Furthmüller J 1996 *Comput. Mater. Sci.* **6** 15
- [18] Kresse G and Furthmüller J 1996 *Phys. Rev. B* **54** 11169
- [19] Shi S Q, Wang D S, Meng S, Chen L Q and Huang X J 2003 *Phys. Rev. B* **67** 115130
- [20] Ceder G, Aydinol M K and Kohan A F 1997 *Comput. Mater. Sci.* **8** 161
- [21] Aydinol M K, Kohan A F, Ceder G, Cho K and Joannopoulos J 1997 *Phys. Rev. B* **56** 1354

- [22] Shi S Q, Ouyang C Y, Xiong Z H, Liu L J, Wang Z X, Li H, Wang D S, Chen L Q and Huang X J 2005 *Phys. Rev. B* **71** 144404
- [23] Yamada A, Takei Y, Koizumi H, Sonoyama N and Kanno R 2005 *Appl. Phys. Lett.* **87** 252503
- [24] Deniard P, Dulac A M, Rocquefelte X, Grigorova V, Lebacqz O, Pastural A and Jobic S 2004 *J. Phys. Chem. Solids* **65** 229
- [25] Nie Z X, Ouyang C Y, Chen J Z, Zhong Z Y, Du Y L, Liu D S, Shi S Q and Lei M S 2010 *Solid State Communications* **150** 40
- [26] Bramnik N N, Bramnik K G, Buhrmester T, Bachtz C, Bhrenberg E and Fuess H 2004 *J. Solid State Electrochem.* **8** 558
- [27] Wolfenstine J, Lee U, Poesche B and Allen J L 2005 *J. Power Sources* **144** 226
- [28] Ni J F, Zhou H H, Chen J T and Zhang X X 2005 *Mater. Lett.* **59** 2361
- [29] Molenda J, Ojczyk W, Świerzek K, Zajac W, Krok F, Dygas J and Liu R S 2006 *Solid State Ionics* **177** 2617
- [30] Le Bacqz O and Pasturel A 2004 *Phys. Rev. B* **69** 245107
- [31] Yamada A, Kudo Y and Liu K Y 2001 *J. Electrochem. Soc.* **148** A1153